

Polyionic Charge Density Plays a Key Role in Differential Recognition of Mobile Ions by Biopolymers

Alexey Savelyev and Garegin A. Papoian*

Department of Chemistry, University of North Carolina at Chapel Hill,
Chapel Hill, North Carolina 27599-3290

Received: February 18, 2008; Revised Manuscript Received: May 17, 2008

We address the question of what are the molecular mechanisms providing discrimination between seemingly similar counterions binding to various biomolecular surfaces. In the case of protein association with Na^+ and K^+ ions, recent works proposed that specificity of carboxylate functional groups interacting with these mobile ions rationalizes the observed ionic discrimination. We probe in this work whether similar arguments may be used to explain higher propensity of Na^+ ions to associate with DNA compared with K^+ ions, which was suggested by our simulations and some experiments. By comparing our extensive molecular dynamics simulations of Na^+ and K^+ distributions around a 16-base-pair DNA oligomer, [(CGAGGTTTAAACCTCG)]₂, with additional simulations where DNA is replaced by a “soup” of monomers (dimethylphosphate anion), we conclude that DNA specificity toward Na^+/K^+ is not determined by the underlying functional group specificity. Instead, the collective effect of DNA charges drives larger Na^+ association. To gain additional microscopic insights into the mechanisms of specificity on ionic associations in these systems, we carried out energetic analysis of the association between Na^+ and K^+ with chloride and dimethylphosphate anions. The insights gained from our computational work shed light on a number of experiments on electrolyte solutions of monovalent salts and DNA.

1. Introduction

Electrolyte solutions provide a ubiquitous medium for functioning of biological macromolecules, such as DNA, RNA and proteins. Numerous prior studies using experimental and computational techniques have revealed the influence of different ionic buffers on the structural and functional behavior of biomolecules. For instance, monovalent counterions mitigate significant electrostatic repulsion between negatively charged DNA base pairs and promote DNA compaction into highly organized structures.¹ This is exemplified by the million-fold DNA compaction into chromatin fiber in the nuclei of eukaryotic cells.^{2,3} The structure, stability and dynamics of the RNA chains are also significantly affected by the salt buffer ionic composition and the counterion condensation details.^{4,5} Mobile ions also mediate the interactions between protein surfaces involved in various cellular processes, such as protein association and aggregation.^{6–8} The question of ionic discrimination in biological systems, thus, arises naturally. For example, competitive distribution of two common monovalent ions, Na^+ and K^+ , around DNA and proteins has been studied extensively by many experimental and theoretical groups during the past decade.^{9–38} The choice of these ions is not surprising - sodium and potassium are the most abundant alkali cations in the living cell. They possess the same charge and differ only slightly in size. It is remarkable, therefore, that the intra- and extracellular concentration ratio of these seemingly indistinguishable ions differs on the order of 10 times.³⁹ Since energy needs to be continuously expended to maintain this large concentration ratio,³⁹ it is clear that ionic selectivity in biological systems is significant or even crucial.

To address the distinct properties of various ions in the living organisms, Collins put forward a model based on the concept of kosmotropic vs chaotropic ionic behavior in a biological environment.^{40–42} Using phenomenological arguments, it has been conjectured that preferential ionic pair formation occurs between oppositely charged ions of roughly the same hydration free energy.^{40–42} When applying this line of reasoning to Na^+ and K^+ , the hydration free energy of sodium was proposed to better match the hydration free energies of the majority of biomolecular anionic groups inside the cell,^{40–42} thus, suggesting stronger association of Na^+ with biomacromolecular surfaces. Since biological macromolecules in a cell function in a very crowded, dense environment, it was argued that the observed large intracellular excess of K^+ ions, which associate less with anionic biomolecules, reduces the potential for unwanted aggregations.^{40–42} In support of these suggestions, a more efficient binding of Na^+ , compared to that of K^+ , to the surfaces of various proteins containing surface COO^- groups, was recently shown.³⁸ The carboxylate group was found to be the dominant attractive site for Na^+ and K^+ ions. The above results were further rationalized in a separate study which demonstrated that Na^+ ions bind stronger to even simple organic molecules containing carboxylate functional group, compared with the K^+ ions.⁴³ Thus, in this case, the specificity of ionic binding to protein surfaces is mainly driven by the specificity of interactions between individual chemical functional groups (carboxylates) and mobile ions (Na^+ or K^+).

Similarly to proteins, Na^+ was proposed to associate with DNA to a significantly larger extent than K^+ .⁴⁴ This suggestion is consistent with a number of experiments on DNA compaction^{45–47} and by measurements of forces between double-stranded DNA chains in sodium and potassium ionic buffers.⁴⁸ However, some other experiments, including NMR spectroscopy and force measurements,^{14,16} did not find substantial differences between

* To whom correspondence should be addressed. E-mail: gpapoian@unc.edu.

Na^+ and K^+ ions. The reasons for discrepancy between various experiments is not currently obvious. Results of these and other relevant experiments will be discussed in Section 3.3. On the basis of all-atom Molecular Dynamics (MD) simulations, we recently proposed several mechanisms of how the ion size regulates the distinct Na^+ and K^+ association.⁴⁴ It is worth noting, that most of the recent computational studies,^{34–36,49–51} motivated by the prior crystallographic and NMR works, investigated in great detail sequence-specific DNA hydration, sequence-specific counterion binding and associated local modulation of the DNA structure (more details and numerous additional citations are given in recent reviews).^{30–32} In addition, most prior all-atom MD simulations were carried out with buffers composed of a single salt, such as a NaCl solution. A few simulation papers comparing the association of Na^+ , K^+ and other alkali metal ions with DNA showed that they differ substantially in their interactions with the DNA sites.^{36,52,53} In particular, detailed analysis of the specific ion-DNA interactions was presented.^{36,53} In contrast, we are interested in the larger picture of the differential Na^+ vs K^+ distribution around DNA, defocusing from the sequence specific details.

In this work, we rationalize the higher Na^+ absorption on DNA chain and suggest a microscopic mechanism determining DNA specificity toward Na^+ and K^+ . In particular, we address the question of whether the stronger Na^+ association is primarily driven by the local, chemically specific interactions with the negatively charged (phosphate) groups, analogous to the carboxylate–cation interactions determining the specificity of protein–ion interactions. To answer this question, we compare the Na^+ and K^+ behaviors in a solution containing either a whole DNA segment or a number of *unconnected* “monomers” derived from DNA backbone. We have studied the Na^+ and K^+ ionic distributions in a system of 30 dimethylphosphate (DMPH) anions, which are directly related to the charged portion of the monomeric unit of the DNA backbone. We carried out a series of extensive all-atom MD simulations using the AMBER force-field of DNA and DMPH systems in explicit water, with equal amount of Na^+ and K^+ neutralizing ions. This is further elaborated in the Computational Method section. The obtained results, which are discussed in Section 3.1, imply that the *collective* action of DNA charges, i.e., the *polymeric* nature of the DNA chain, drives larger Na^+ association, as opposed to the effect being driven by chemically specific interactions with the phosphate group. Thus, polyionic charge density plays a crucial role in ionic recognition. In a related prior work, Vaitheeswaran and Thirumalai have shown that ionic charge density of mobile spherical ions in water nanodroplets determines the extent of interior solvation and the interionic interaction free energy profile.⁵⁴ Charge-density of DNA and counterions also influences the extent of mobile ion–ion correlations near the DNA surface. Differential stabilization of ions of different size due the latter effect is another factor modulating ionic recognition.

Similar simulations carried out in CHARMM also support this trend, although the difference between Na^+ and K^+ association with DNA is significantly smaller in CHARMM. Our findings demonstrate that the idea of separating the ions into kosmotropes and chaotropes does not fully characterize the problem of ion-biomolecule interactions: while it may work for many proteins, other considerations, such as the polyionic charge density effect, discussed in this work, are also important to describe specificity in DNA-electrolyte solutions.

Another goal of this study is to gain a more microscopic understanding of a differential character of Na^+ –DNA and

K^+ –DNA interactions in *halide-containing* DNA systems, studied previously, where K^+ counterions were found to be screened more efficiently than Na^+ counterions by Cl^- coins from DNA.⁴⁴ In such systems the difference between Na^+ and K^+ association with DNA is even more pronounced. To address the interplay between coion-counterion (Na^+ – Cl^- , K^+ – Cl^-) complexation and the DNA–counterion interactions, we performed a comparative analysis between energetics of Na^+ and K^+ association with the chloride and DMPH anion, a “monomeric” building block of the DNA. As mentioned above and discussed in Section 3.2, DMPH anion exhibits very low selectivity with respect to Na^+ and K^+ . Therefore, we set to investigate what leads to an enhancement of this selectivity as DMPH anion is replaced by Cl^- . Our approach is based on the approximate calculation of the entropic and energetic contributions to the free energy change upon ionic pair formation, complementary to the analysis of the ionic distribution profiles in Section 3.1. This technique allows us to elucidate the microscopic mechanisms of differential ionic pair formation between Na^+ and K^+ with Cl^- and DMPH anions.

In summary, the findings of the present work, combined with our earlier results,⁴⁴ provide a thorough picture of the competitive Na^+ vs K^+ association with DNA in systems with and without corresponding halides. The results of the first part of this work (Section 3.1) indicate that: (1) In a halide-free solution of unconnected DMPH anions, K^+ binds with slightly higher propensity, than Na^+ , to the DMPH ion. (2) In a halide-free DNA solution, Na^+ binds with higher propensity, indicating that *cooperative* effect of numerous charges on DNA produces a locally enhanced electrostatic field, which, in turn, acts to reverse the chemical specificity of slightly stronger K^+ –phosphate interactions. This DNA polyionic charge density effect may be considered as a mechanism, complementary to those suggested in our prior work,⁴⁴ of higher Na^+ association with DNA. In addition, the energetic analysis of the Na^+ and K^+ complexation with Cl^- and DMPH anion (Section 3.2) provides a microscopic explanation of the markedly different extent of ionic pair formation in halide and DMPH systems. This rationalizes the more pronounced difference between Na^+ and K^+ association with DNA in a halide-containing, compared to halide-free, DNA systems. It is shown that because of a lower dehydration penalty for larger K^+ ions, the latter associates more readily with Cl^- , than Na^+ . In difference, ionic dehydration does not play a decisive role in DMPH solution, and DMPH ions exhibit virtually no selectivity toward Na^+ and K^+ .

The issue of force field adequacy is critically discussed at the end of Section 3.2. The main conclusions of this work, discussed in the previous paragraph, are in qualitative agreement with a number of independent experimental studies on DNA in various monovalent counterion buffers, as well as with experimentally measured activity coefficients in different electrolyte solutions, as elaborated in Section 3.3. Further studies are needed to clarify why other experiments based on the NMR spectroscopy and force measurements show insignificant difference between Na^+ and K^+ buffers.

2. Computational Methods

2.1. Analysis of Counterion Distribution around DNA and DMPH Ions. 2.1.1. MD Simulation Protocol. One of the central questions of our work is whether enhanced attraction of Na^+ to DNA, compared with K^+ , is a collective effect, due to the polyionic character of DNA, or is simply based on chemical specificity of counterion interaction with individual functional groups, such as phosphates. To address this question, we simulated and analyzed

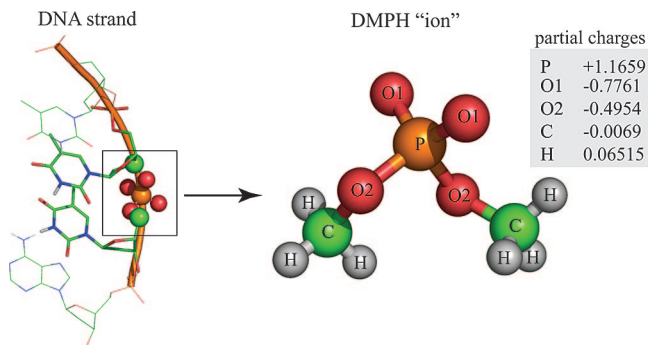


Figure 1. Dimethylphosphate (DMPH) ion, $(\text{CH}_3)_2\text{PO}_4^-$ (on the right), was obtained by adding hydrogens, to complete the valence of carbon atoms, to the $(-\text{C}-\text{PO}_4^--\text{C}-)$ functional group, “clipped out” from the DNA strand backbone (shown on the left). Partial charges of the DMPH anion atoms are provided in units of the electron charge.

the following two systems: (1) the DNA 16-mer, neutralized by Na^+ and K^+ ions, in an aqueous solution; and (2) 30 individual DMPH ions, each carrying a -1 charge, neutralized by Na^+ and K^+ ions, in an aqueous solution. The DMPH represents the charged segment of the DNA backbone monomeric unit. DMPH parametrization details are discussed below. In what follows, we shall refer to the above systems as **1** and **2**, respectively. The starting point for simulations **1** and **2** were a canonical B-form of a 16-base-pair DNA oligomer, $[\text{d}(\text{CGAGGTTTAAACCTCG})]_2$, and a DMPH ion, respectively. We built an ideal DNA chain and the DMPH ion models and carried out all-atom MD simulations in explicit, TIP3P water⁵⁵ using the AMBER 8.0 suite of programs⁵⁶ and the AMBER Parm99 force-field.⁵⁷ The initial structures in all systems were first neutralized by 15 Na^+ and 15 K^+ ions. The initial positions of the ions were determined from the computed electrostatic potential using the software package LEaP.⁵⁶ System **1** was simulated in our prior work:⁴⁴ here we reanalyzed the previously obtained trajectory. System **2** was further solvated in more than 6000 TIP3P water molecules in a cubic box, having dimensions $60 \times 60 \times 60 \text{ \AA}^3$. The overall number of atoms in each system was $\sim 19\,500$ in the periodic box. We used a multistage equilibration process, reported by Orozco and co-workers,⁵⁸ to equilibrate all starting structures. The subsequent production runs for MDs in all systems were carried out at constant temperature (300 K) and pressure (1 bar) using the Langevin temperature equilibration scheme (see AMBER 8 manual), the “weak-coupling” pressure equilibration scheme,⁵⁹ and periodic boundary conditions.

The translational center-of-mass motion was removed every 2 ps. We used the SHAKE algorithm⁶⁰ to constrain all bonds involving hydrogens, which allows all MD simulations to use an increased time step of 2 fs without any instability. Particle Mesh Ewald method⁶¹ was used to treat long-range interactions with a 9 \AA nonbonded cutoff. The production runs for simulations in **1** and **2** were carried out for 60 ns to ensure the equilibration of ions. It was shown in prior works^{35,36} that 50 ns MD was enough to equilibrate the Na^+ atmosphere around DNA in a smaller system comprised of $\sim 16\,000$ atoms. Given the slightly larger size of our systems ($\sim 19\,500$ atoms), we used extra 10 ns of MD to ensure equilibration.

2.1.2. Parameterization of the DMPH Anion. The chemical structure of the DMPH ion, which is the anion simulated in system **2**, is given in the Figure 1. The basic monomeric unit of the DNA backbone contains a negatively charged phosphate functional group, connected with two sp^3 carbon atoms. When “clipped out” of the DNA backbone, it is necessary to add hydrogens to these carbons, to complete the valency of individual DMPH ions. The bond, angle and dihedral potential parameters for the DMPH ion, as well as the partial charges for 13 atoms in the clipped phosphate group, were taken from the corresponding portion of DNA parametrization in the AMBER Parm99 force-field. The partial charges were slightly modified, using symmetry considerations and from the requirement for the net charge of the DMPH ion to be -1 , to take into account morphing of carbon atoms to methyls.

2.1.3. Computing the Ion–DNA and Ion–DMPH Ion Radial Distribution Functions. To analyze in detail the Na^+ and K^+ distributions around the DNA segment in **1** and the DMPH ion in **2**, we calculated their radial distribution functions (RDF).⁶² All RDFs were based on first defining the DNA–counterion and the DMPH–counterion distances as the *closest* distances between the molecule of interest and the particular counterion. These distances were used to construct DNA–ion and DMPH–ion distance histograms from each snapshot of the MD simulation. To obtain the RDFs, the histograms need to be normalized by the volume Jacobian.⁶² Indeed, the number of neighbors within a distance r from a given object is

$$n(r) = \rho \int_0^r g(r) J(r) \, dr \quad (2.1)$$

where ρ is the average particle concentration, $g(r)$ is the RDF (pair correlation function) and $J(r)$ is the volume Jacobian. We

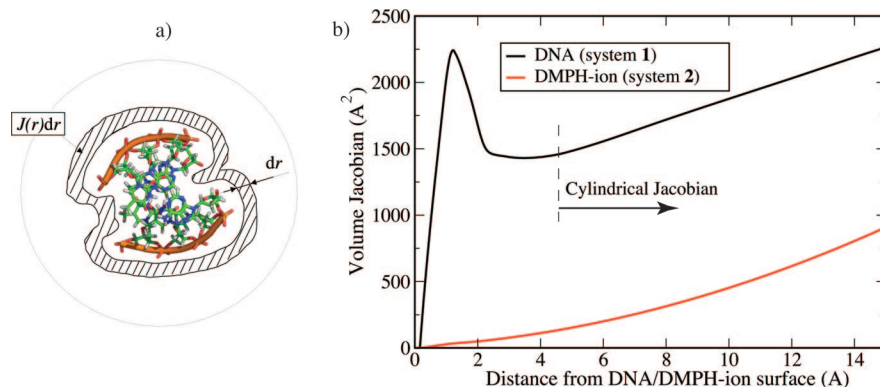


Figure 2. (a) Top view of the DNA segment and an equidistant shell from its surface (dashed region). (b) Numerical volume Jacobian for the DNA segment (black) and the DMPH ion (red) as a function of the distance from the DNA and the DMPH ion surface, correspondingly. For the DMPH ion, whose shape is close to a sphere, the Jacobian is a monotonically increasing function; in contrast, for the DNA oligomer, the function is monotonically increasing only after $\sim 4 \text{ \AA}$ from its surface, where it can be approximated as a cylindrical Jacobian. This is caused by the complex and irregular shape of the macromolecule, as indicated in panel (a).

defined the latter as the volume of a shell, equidistant from the DNA or DMPH ion surfaces (see Figure 2a).

The volume Jacobians were numerically calculated as a function of a distance from the DNA and the DMPH ion surfaces (Figure 2b). The present method of computing $J(r)$ differs from the standard procedure of calculating either the spherical (see *ptraj* utility of the AMBER package) or the cylindrical Jacobians for DNA (as used in ref 35). Although, DNA is on average cylindrically symmetric, and the use of the cylindrical Jacobian is reasonable, the latter techniques lead to an overestimation of the counterion association at small distances from the DNA surface. This is important, in particular, when calculating the absolute number and ratio of ions contributing to the various RDF peaks (see below). While the numerical volume Jacobian for DMPH ion is a monotonically increasing function (DMPH's shape is close to a sphere), the Jacobian for the DNA segment, taking into account its complex and irregular shape (see Figure 2a), is characterized by an unusual *nonmonotonic* behavior in the vicinity of the DNA oligomer (Figure 2b). It is seen that only at distances more than ~ 4 Å from DNA surface the monotonically increasing Jacobian can be approximated by the cylindrical one. Ion–DNA and ion–DMPH distance histograms, computed over the MD simulation course for every snapshot, were normalized by the corresponding numerical Jacobians. Three-dimensional grids with a lattice spacing of 0.25 Å were used to calculate the ion–DNA, the ion–DMPH distance histograms and the volume Jacobians. The biochemical algorithm library (BALL)⁶³ was used to implement the computational analysis subroutines.

2.2. Analysis of the Free Energy Change upon Na⁺ and K⁺ Association with Cl⁻ and DMPH Ion. Another question of this study is to elucidate which microscopic interactions are responsible for the different extent of Na⁺ and K⁺ complexation with Cl⁻ and DMPH ion, and, thus, to further rationalize the higher screening of K⁺ by Cl⁻ in halide-containing DNA systems studied recently.⁴⁴ We address this issue by calculating and analyzing the free energy difference between bound and unbound states for the corresponding pair of oppositely charged ions—Na⁺ and Cl⁻, K⁺ and Cl⁻, Na⁺ and DMPH, and K⁺ and DMPH—in an aqueous solution. These four systems, each comprised of the corresponding ionic pair solvated in explicit (TIP3P) water, were simulated in AMBER force-field according to the MD protocol described in Section 2.1.1. The halide and DMPH systems were solvated in ~ 600 and ~ 1000 TIP3P water molecules in a cubic boxes, having dimensions $27 \times 27 \times 27$ and $34 \times 34 \times 34$ Å³, respectively. We define the unbound state for the pair of ions if the distance between their surfaces is 12 Å and more. This threshold was estimated from the ion/water RDF and corresponds to the regime when the first two hydration shells of neither of ions are perturbed. Hence, almost twice as larger size of Na⁺–DMPH and

K⁺–DMPH systems is caused by the larger size of DMPH molecule, compared to Cl⁻. Note that the above threshold exceeds almost twice the electrostatic screening length (Bjerrum length) which for our simulated conditions is ~ 7 Å. Therefore, the ions in the unbound state interact with an energy significantly less than the thermal energy. On the other hand, two ions were considered to be associated if they were found at a distance of less than certain threshold, which correspond to the trough between the first (direct ionic binding) and second (water-mediated pair) peaks in the ion/ion RDF. Details on computing the energetic and entropic contributions to the free energy difference are provided below.

2.2.1. Estimation of Free Energy, Energy, and Entropy Differencies. The free energy difference upon ionic association can be computed in a number of ways, for example, by calculating the potential of mean force (PMF) for bringing to proximity two ions; then, the free energy of association could be estimated from the difference between PMF integrated over the range of distances, corresponding to large and small ionic separations (see, e.g., ref 64 and references therein). Alternatively, the free energy difference can be expressed through the ratio of occupation of states,

$$\Delta F = -k_B T \ln \frac{p_2}{p_1} \quad (2.2)$$

where p_1 and p_2 correspond to the number of events when ions are free and associated, respectively. Provided that system is well-equilibrated (productive runs of our simulations are ~ 100 ns for each system of solvated ionic pair) and enough bound/unbound events are observed to obtain converged statistics, eq 2.2 can be used to compute the free energy differences in systems of solvated ionic pairs directly from MD simulations.⁶⁵

More detailed information about energetic and entropic contributions to the free energy, $\Delta F = \Delta E - T\Delta S$, can be obtained by computing an average potential energy difference, ΔE , between associated and free ionic states. Next, we assume that the entropy change between two ionic states, ΔS , includes two contributions: 1) the entropy gain of the water molecules, ΔS_{wat} , released from the first and second ionic solvation shells due to ionic binding, and 2) the loss of translational entropy of the ions, ΔS_{ion} , for the same reason. The latter contribution can be estimated from the following simple expression,

$$\Delta S_{ion} = k_B \ln \frac{V_{pair}}{V_{free}}, \quad V_{pair} = \frac{4}{3}\pi(R_2^3 - R_1^3),$$

$$V_{free} = V_{box} - \frac{4}{3}\pi R_{ex}^3 \quad (2.3)$$

reflecting the fact that upon the binding a given ion is confined within the accessible volume, V_{pair} , around the other ion it binds

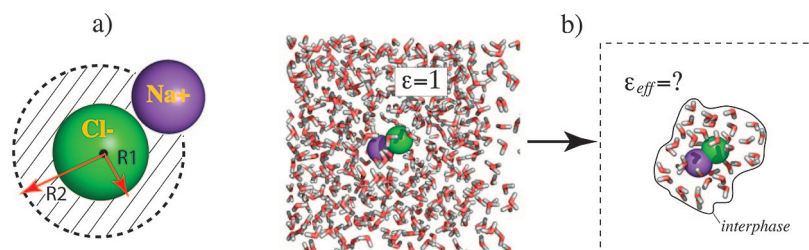


Figure 3. (a) Dashed region is a volume V_{pair} [see eq 2.3], accessible for an ion (Na⁺) upon its binding to an oppositely charged ion (Cl⁻). Distances R_1 and R_2 are taken from the corresponding ion/ion RDF. (b) Mean-field (MF) approximation for calculation of the system energy change upon ionic binding. As a result of MF approach, the associated Na⁺ Cl⁻ pair in explicit water ($\epsilon = 1$) in a simulation box (on the left) is partitioned into explicit region, the hydrated ions, and the continuous medium with an effective permittivity, ϵ_{eff} (on the right). See the text for details.

to (see Figure 3a). The threshold distances, R_1 and R_2 , were taken from the RDFs computed for the corresponding ionic pairs. The volume V_{free} is the volume accessible for an ion in the unbound state, which is the difference between the volume of the periodic boundary cell, V_{box} , and the volume of a sphere of radius $R_{ex} = 12 \text{ \AA}$, the latter is the threshold distance defining the unbound state (see above). Then, the ratio V_{pair}/V_{free} relates to the entropy loss of an ion upon binding. Finally, given ΔF (eq 2.2), ΔE and ΔS_{ion} (eq 2.3) one can compute the entropy gain, ΔS_{wat} , of solvent molecules released to the bulk upon ionic binding. It will be shown in Section 3.2 that this information, along with the known experimentally measured entropy of water at the melting point, can be used to roughly estimate the absolute entropy of a single water molecule residing in the first and/or second solvation shell of Na^+ and K^+ ions.

2.2.2. Detailed analysis of the energetic contribution from the mean-field approach. The change of the system's total potential energy, ΔE , due to ionic association gives only one number and does not provide an information about the energetic role of each system constituent—water molecules and ions. The latter can be elucidated by computing from simulations the average changes of Coulombic and van der Waals contributions to the total potential energy difference, according to the system Hamiltonian,

$$H = \sum_{i < j} \left[\frac{q_i q_j}{\epsilon_{eff} R_{ij}} + 4\epsilon_{ij} \left\{ \left(\frac{\sigma_{ij}}{R_{ij}} \right)^{12} - \left(\frac{\sigma_{ij}}{R_{ij}} \right)^6 \right\} \right] \quad (2.4)$$

for solvent–solvent, ion–solvent and ion–ion interactions. Here i, j denote the atom indices, R_{ij} is the distance between the particular pair of atoms, q_i is the particle charge, ϵ_{eff} is the effective dielectric constant of the medium (see below), and ϵ_{ij} and σ_{ij} are the parameters of the Lennard–Jones potential computed by Lorentz–Berthelot combination rules⁶⁶

$$\epsilon_{ij} = \sqrt{\epsilon_i \epsilon_j}, \quad \sigma_{ij} = \frac{\sigma_i + \sigma_j}{2} \quad (2.5)$$

Parameters $\sigma_{i,j}$ and $\epsilon_{i,j}$ in the last equations were taken from the corresponding parametrization of the Lennard–Jones potential in the AMBER Parm99 force-field. We used Hamiltonian eq 2.4 to study both halide and DMPH systems. In the latter systems we do not account for the bond, angle and dihedral energetic terms since they give much smaller contribution to the free energy of association, compared to electrostatic and van der Waals energies.

As an approximation, we computed Coulombic and van der Waals contributions only for the ions and the solvent molecules, participating in the first and second ionic solvation shells, whereas the rest of solvent was treated as a continuous medium with an *effective* dielectric constant ϵ_{eff} (see below). This is indicated by the prime at the sum in eq 2.4, denoting a summation over the specified region around each ion or pair of associated ions. The proposed *mean-field* model is schematically depicted in the Figure 3b. The corresponding energetic differences computed in the way described above allowed us to compare the electrostatic gain for ionic association and the electrostatic loss due to ionic dehydration penalty. Other contributions, such as self-energy of the solvent molecules within the first and second ionic solvation shells, are also easy to analyze. In other words, decoupling the contributions of solvent and ions from each other is the way to elucidate which of them has the largest impact on the ionic association.

Next we describe the way we estimated the effective permittivity, ϵ_{eff} , where the solvent beyond the explicitly defined region around the ions is treated using the mean-field approach.

We determined ϵ_{eff} by comparing the computed, in accordance with eq 2.4, Coulombic part of the energy difference (with $\epsilon = 1$), ΔE_{Col} , and the average electrostatic energy difference, ΔE_{el} , extracted directly from simulation output file. Since the latter is an exact result obtained when *all* atoms were treated explicitly, ϵ_{eff} is just the scaling factor to the approximate mean-field difference ΔE_{Col} , such that $\Delta E_{Col} \approx \Delta E_{el}$. The value of effective permittivity was estimated to be $\epsilon_{eff} \approx 2$ for our simulations of the halide systems. The physical plausibility of this value of ϵ_{eff} is discussed below. As for the DMPH systems, an analogous estimation of ϵ_{eff} turned out to be too noisy, due to insufficient statistics of ion pairing to obtain sufficiently well converged potential energy averages, despite relatively long simulation times. Therefore, we used the same value of $\epsilon_{eff} \approx 2$ to scale electrostatic interactions in DMPH systems.

Finally, it has to be pointed out that the above scaling with ϵ_{eff} produces an *effective* electrostatic energy, possessing both energetic and entropic contributions (thus, a free energy). Therefore, our mean-field analysis of different energy contributions, as explained in this section, implies that the formal decomposition of the free energy into purely entropic and energetic parts (see above) is an approximation itself. In addition, although two layers of water included in the explicit region is expected to be sufficient, extending the explicit region further will probably improve accuracy. Despite these issue, our analysis provides useful qualitative insights into the specific electrostatic interactions that favor various ionic associations, as elaborated below.

3. Results and Discussion

3.1. Comparing Counterion Distributions in DNA and DMPH Systems. To compare the differential tendency for the Na^+ and K^+ ions to bind to an oppositely charged solute molecule, the DNA oligomer in system **1** and the DMPH ion in system **2**, the corresponding ion–solute RDFs were computed from MD simulations (see Figure 4). Since the numbers of the Na^+ and K^+ ions were equal in both simulated systems, the RDF functions provide direct information on competitive binding.

The simulation of system **1** produced significantly larger Na^+ association in the immediate vicinity of the DNA oligomer compared with K^+ (Figure 4a). On the other hand, at distances greater than $\sim 8 \text{ \AA}$ from the DNA segment, corresponding to the third RDF peak and beyond, both Na^+ and K^+ ions were found with a similar frequency. Sodium and potassium distribution profiles around DNA in a halide-free system was reported and partially rationalized in our prior work.⁴⁴ We suggested that two mechanisms are responsible for the observed dissimilarity of Na^+ and K^+ distributions around DNA: (1) smaller Na^+ ions, when partially dehydrated, can penetrate the DNA core more easily; and (2) smaller Na^+ ions approach closer to the DNA surface, experience larger, attractive electrostatic potential. These effects work cooperatively to enhance Na^+ association compared to K^+ . In particular, they rationalize the higher and closer to DNA Na^+ RDF first peak, indicating stronger absorption of Na^+ on DNA and an enhanced attraction by interacting with stronger DNA electrostatic field.

Following the reasoning above, one might hypothesize that the polyionic nature of DNA, in particular locally enhanced charge density, plays an important role in controlling ionic specificity. Enhanced Na^+ binding to DNA could be partially driven by strong electrostatic field created collectively by the DNA negative charges positioned on the phosphate groups. If this conjecture is valid, then one would expect that in a system

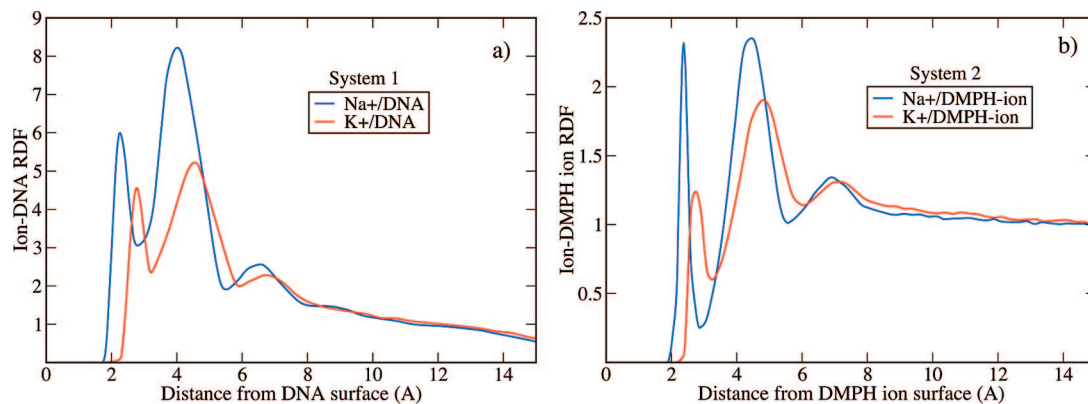


Figure 4. Na⁺/DNA (blue) and K⁺/DNA (red) radial distribution functions computed from simulations of (a) DNA system **1** and (b) DMPH system **2**.

TABLE 1: Ratios of the Na⁺ to K⁺ Ions Contributing to the First Peak and to the First Three Peaks of the Ion/DNA and Ion/DMPH Ion RDFs, Computed for DNA System **1 and a System **2** of Broken DMPH “monomers”^a**

	system 1 (DNA)		system 2 (DMPH)	
	first peak	three peaks	first peak	three peaks
Na ⁺ /K ⁺	1.34	1.2	0.9	1.04

^a Bold values indicate qualitatively different character of the *direct* ionic binding to DNA in **1** and to DMPH ion in **2** with the prevalence of Na⁺ in the former system and the slight prevalence of K⁺ in the latter system. Note that the phrase “direct binding” is used here in a somewhat different meaning from what is usually considered when computing, for example, association binding constants.

of unconnected monomers, that represent the DNA backbone repeating unit, the Na⁺ and K⁺ would show more similar propensities to condense around the anionic monomers.

To verify this hypothesis we investigated system **2**, which consisted of 30 DMPH anions. The simulations details using the AMBER force-field are described in the Methods Section. The calculated Na⁺/DMPH ion and K⁺/DMPH ion RDFs are shown in the Figure 4b. Similar to system **1** with DNA, the most prevalent DMPH-anion binding sites for both Na⁺ and K⁺ turned out to be negatively charged O1, O2 atoms (see Figure 1) of the phosphate group. We estimated the extent of sodium and potassium association with DNA and DMPH ion in **1** and **2**, respectively, by calculating, using eq 2.1, the ratios of the Na⁺ to K⁺ ions contributing to the first three RDF peaks (within a radius of ~9 Å) from DNA and DMPH ion surfaces. This region is formally considered to coincide with the Manning radius²¹ of ~9 Å in counterion condensation theory, although the latter is strictly valid in the limit of infinitely long line, instead of cylindrically shaped DNA of finite length. Nevertheless, the fraction of DNA charge, neutralized by counterions, was predicted to be around ~76% by counterion condensation theory and was confirmed by the all-atom MD simulations^{35,44} and by experimental measurement of forces between double-stranded DNA chains⁴⁸ (see Section 3.3). In addition, we examined the extent of *direct binding* of ions to solute molecule by calculating the ratios of the Na⁺ to K⁺ ions contributing to the first RDF peaks: a direct interaction between DNA/DMPH ion and a counterion corresponds to the distance between them of less than 2.87 Å for Na⁺ and 3.35 Å for K⁺ ions. Table 1 summarizes both ratios in systems **1** and **2**.

Table 1 results indicate qualitatively different ionic binding in two systems: the character of direct binding changes dramatically from sodium dominance by 34% to potassium dominance by 10%

(see bold values in the Table 1) as one passes from the double-stranded DNA chain in **1** to its “monomeric” analogue, the DMPH ion, in **2**. To avoid misunderstanding, it should be noted that by “direct binding” here we do not mean a process characterized by a *binding constant*, *K*, as customary. The latter can be computed through the RDF integrated over the whole range of distances between molecules of interest - from their contact to the infinite separation. Instead, we are interested in the ratios of the sodium and potassium ions contributing to different RDF peaks to characterize their distribution in the vicinity of the solute molecule, where ions are structured with respect to DNA/DMPH anions. The contributions of Na⁺ and K⁺ ions to a region of 9 Å from the solute molecule also change noticeably as DNA is replaced by DMPH anions: as we hypothesized, the pronounced Na⁺ prevalence of ~20% in DNA system reduces to small Na⁺ dominance of ~4% in DMPH system, indicating a more similar propensities for Na⁺ and K⁺ to condense around the DMPH-anions. Hence, we conclude that, in addition to the above-mentioned mechanisms, a significant DNA polyionic charge density effect favors sodium ions.

Despite the above-mentioned difference between the usual way of characterizing the ionic binding and our approach here, focused on RDF peaks, we can still approximately estimate the relative Na⁺ to K⁺ binding free energies in systems **1** and **2**. For that we use the data of Table 1 for the ratio of ions contributing to the first three RDF peaks. This results in free energy differences, $\ln(1.2) \approx 0.2$ kT and $\ln(1.04) \approx 0.04$ kT, for systems **1** and **2**, respectively. Such rather small values might raise a question of the force-field specificity of the obtained results, particularly, if the observed trend Na⁺ > K⁺ in the binding affinity to DNA in system **1** is significantly reduced in system **2**, where DNA is replaced with a “soup” of DMPH anions. To investigate this issue, we repeated the MD simulations for systems **1** and **2** (with an equivalent MD simulation protocol), using the CHARMM27 force-field^{67,68} which, along with AMBER, is among the most commonly used all-atom force-fields. It turned out that Na⁺ ions still associate with DNA to a larger degree compared to K⁺, albeit with reduced specificity (by ~5% within 9 Å from DNA surface, compared with ~20% in AMBER simulation). On the other hand, the difference in Na⁺ and K⁺ binding to DMPH anion appeared to be negligible, which confirms that CHARMM force-field also captures the influence of the DNA polyionic effect on the specificity between Na⁺ and K⁺ ions, the main result of this work.

3.2. Energetic Analysis of Na⁺ and K⁺ Association with Cl⁻ and DMPH Ions. Following the technique described in the Computational Methods section, we calculated and analyzed the free energy differences for Na⁺ and K⁺ ions to associate

TABLE 2: Free Energy and the Corresponding Energy and Entropy Differences between Associated and Unbound States for $\text{Na}^+ - \text{Cl}^-$ and $\text{K}^+ - \text{Cl}^-$ Ionic Pairs^a

	ΔF	ΔE	$-T\Delta S$	ΔS		no. of released waters	
				ΔS_{ion}	ΔS_{wat}	first shell	second shell
NaCl	1.37	1.57	-0.2	-4	4.34	3.2	20
KCl	0.45	-0.2	0.65	-3.87	3.5	3.5	20

^a ΔF , ΔE , and $T\Delta S$ are given in kcal/mol, entropies are in units of k_B (Boltzmann constant). Numbers of water molecules are given for those released from the first and second ionic solvation shells upon ionic binding. For details, see the Computational Methods section.

with Cl^- and DMPH anions. As mentioned above, we performed this comparative analysis to further rationalize the observed in our prior study interplay between the coion-counterion complexation and the counterion-DNA interactions in the halide-containing DNA systems.^{44,69} Since the question of the influence of DNA polyionic nature on the competitive Na^+ vs K^+ association was answered in the previous Section, we focus here on the energetics of Na^+ and K^+ interactions with the DNA monomeric unit, the DMPH anion, and compare the obtained results with those for Na^+ and K^+ interactions with Cl^- . To this end, we simulated four small systems, each comprised of the corresponding pair of ions solvated in explicit water, and calculated free energy change and the corresponding energy and entropy contributions upon ionic binding, as elaborated in the Computational Methods section. We first present the data obtained for halide systems, followed by the results for DMPH solutions.

Free energy differences between associated and unbound states for $\text{Na}^+ - \text{Cl}^-$ and $\text{K}^+ - \text{Cl}^-$ pairs of ions, along with the corresponding energetic and entropic contributions, are given in the Table 2. The obtained data indicate that the free energy penalty for ionic binding is higher for NaCl solution; it is caused mainly by the significant increase of the energy of interactions in NaCl solution. In difference, in KCl solution the energetics favors K^+ and Cl^- association, whereas the entropy part of the free energy difference prohibits ionic binding. Interestingly, the energy and entropy reverse signs as one passes from NaCl to KCl solution. To understand this we explored both contributions as elaborated in the Method section.

We start by discussing the entropy change. As indicated in Table 2 the entropy loss due to ionic binding is roughly the same in NaCl and KCl systems, since it is determined by the radii of ions only. On the other hand, the entropy gains coming from the water release when ions associate differ substantially in NaCl and KCl solutions, resulting in a different signs of $T\Delta S$ contributions. A higher ΔS_{wat} in NaCl system is not surprising, since smaller Na^+ ion interacts more strongly (electrostatically) with surrounding water molecules, restricting stronger their mobility. Thus, water molecules acquire larger entropy gain when released from the Na^+ solvation shell. Particularly, the entropy increase per water molecule released from the first solvation shell upon $\text{Na}^+ - \text{Cl}^-$ association may be estimated as $4.3/3.2 \approx 1.35k_B$, compared with $3.5/3.2 \approx 1.1k_B$ for the KCl association. We assumed here that the main entropy gain originates from first shell water molecules. These results are in agreement with the expectation that potassium's water molecules possess higher entropy due to weaker $\text{K}^+ - \text{water}$ electrostatic interactions.

We discuss next the energetic part of the free energy difference for ionic association. To find out what type of

TABLE 3: Differences between Electrostatic and van der Waals Energy Changes in NaCl and KCl Solutions upon Ionic Binding Were Computed As Explained in the Computational Methods Section^a

	electrostatic			van der Waals		
	$\Delta\Delta E^{ii}$	$\Delta\Delta E^{is}$	$\Delta\Delta E^{ss}$	$\Delta\Delta E^{ii}$	$\Delta\Delta E^{is}$	$\Delta\Delta E^{ss}$
NaCl - KCl	-5.75	11.65	-3.65	0.05	-0.66	-0.17

^a Electrostatic energies are scaled with effective permittivity, $\epsilon_{eff} = 2$ (see the text). “*ii*”, “*is*” and “*ss*” stand for ion-ion, ion-solvent and solvent-solvent interactions. All values are in kcal/mol.

interactions are responsible for the observed energy differences (Table 2) one needs to analyze the energetic role of each system constituent upon ionic binding. As elaborated in the Computational Methods section, we propose to use the *mean-field* approximation to calculate all (six) type of system interactions, which are the Coulombic and van der Waals ion-ion, solvent-ion and solvent-solvent interactions, according to the system Hamiltonian, eq 2.4. Since in the following analysis the majority of solvent is treated implicitly, it is reasonable to consider not the change in different energetic contributions upon ionic binding for each system separately, but the corresponding differences between these contributions for NaCl and KCl systems. Indeed, partitioning the system into the explicit part (ions with their first and second solvation shells) and the continuous surrounding medium does not account for the energy of interactions of the water molecules, released upon ionic binding, with the rest of the system; similarly, their self-energy is also not considered. However, as in both halide systems there are roughly an equal numbers of water molecules released (~ 20 , see Table 2), these unaccounted contributions cancel out when differences between NaCl and KCl energy changes are considered.

Table 3 provides the detailed energetic data calculated from MD simulations of NaCl and KCl systems. It is seen that, as ions associate, all contributions to the van der Waals energy change are about the same in both halide systems. The unequal energy of electrostatic interactions play major role in the different Na^+ and K^+ binding to Cl^- . The latter, as explained in the Methods section, needs to be scaled by the effective dielectric constant, ϵ_{eff} , which emerges from the mean-field treatment of the solvent outside of the specified region. To show that the obtained $\epsilon_{eff} \approx 2$ is a physically reasonable value, we refer to a simple estimate of effective permittivity for a protein ($\epsilon_1 \approx 3$) in water ($\epsilon_2 \approx 80$), yielding the values of ϵ_{eff} in a range of $[\epsilon_1 \dots (\epsilon_1 + \epsilon_2)/2]$, or $[\approx 3 \dots 40]$ (see, e.g. ref 70). Here, the lower boundary corresponds to the case when the distances between charges are much less than the distance between the charge and the water/protein interface, and the upper limit corresponds to large distances between charges. In our case, a “protein” corresponds to explicit part of the system—the hydrated ion or pair of ions, with $\epsilon_1 = 1$. Hence, the obtained value $\epsilon_{eff} \approx 2$, close to the lower limit, reflects that, on average, the distances between charges within explicit domain are less than distance from charges to the hydrated-ion/continuous-media interface.

The largest difference between NaCl and KCl energy changes comes from the ion-water electrostatic interactions (Table 3), indicating much stronger interactions between an *unbound* cation and the water molecules in its hydration shell in NaCl system. This, on the one hand, leads to a higher energetic penalty for water molecules released from the sodium's solvation shell upon $\text{Na}^+ - \text{Cl}^-$ association. On the other hand, it results in an overall

TABLE 4: Differences between Electrostatic and van der Waals Energy Changes in Na–DMPH and K–DMPH Solutions upon Ionic Binding Were Computed As Explained in the Computational Methods Section^a

	electrostatic			van der Waals		
	$\Delta\Delta E^{ii}$	$\Delta\Delta E^{is}$	$\Delta\Delta E^{ss}$	$\Delta\Delta E^{ii}$	$\Delta\Delta E^{is}$	$\Delta\Delta E^{ss}$
Na(DMPH) – K(DMPH)	–12.78	21.24	–7.72	1.2	–2.41	0.86

^a Electrostatic energies are scaled with effective permittivity, $\epsilon_{eff} \approx 2$, derived for halide systems. “*ii*”, “*is*” and “*ss*” stand for ion–ion, ion–solvent and solvent–solvent interactions. All values are in kcal/mol.

entropy-increase in Na⁺ Cl[–] system (see Table 2), although the latter does not play a decisive role. Note that the electrostatic ion–water contribution—the ion’s dehydration penalty—is larger than both the ion–ion and water–water contributions combined, the latter two favoring more sodium’s, than potassium’s, complexation to Cl[–]. Particularly, the overall electrostatic energy change is positive and larger by 2.5 kcal/mol for Na⁺–Cl[–] binding, relative to that for K⁺–Cl[–] association; it is entirely caused by the higher dehydration penalty of smaller Na⁺ ion. Since the van der Waals energy changes insignificantly in both halide systems (see Table 3), we conclude that the reason of different Na⁺ and K⁺ association with Cl[–] is a different dehydration penalty of cations, regulated by the ion size.

Similar analysis performed for Na–DMPH and K–DMPH systems did not reveal a noticeable difference between the free energy changes upon Na⁺ and K⁺ association with DMPH anion. The free energy change in both DMPH solutions was estimated to be ~ 4.5 kcal/mol, consequently, significantly less binding events were observed compared to halides. Mainly because of this, we were unable to get a reliable data on the energetic changes upon Na⁺ and K⁺ association with DMPH anion: by calculating the total energy changes upon ionic binding, averaged over different parts of the MD trajectory, we came to conclusion that DMPH systems are not nearly enough equilibrated, despite the relatively long simulation time (120 ns). Therefore, we avoid the discussion of the data for DMPH systems analogous to those presented in the Table 2 for halide systems. Nevertheless, the ratios of bound to unbound ionic states, i.e., the free energy differences in both systems, appeared steady with increasing simulation time.

The lack of statistical convergence in DMPH systems, however, does not make impossible a qualitative energetic analysis of Na⁺ and K⁺ association with DMPH anion (in a way we did it for halides, see Table 3) to reveal at least the relative energetic affinity of Na⁺ and K⁺ to bind to DMPH anion. The data for the corresponding differences between electrostatic and van der Waals energy changes for Na(DMPH) and K(DMPH) systems are presented in the Table 4. We used the value of $\epsilon_{eff} \approx 2$ for effective dielectric permittivity, calculated for halide systems, to scale the electrostatic interactions. As in case of halides, various van der Waals interactions do not change dramatically. The amplitudes of electrostatic energy changes are considerably higher and electrostatics, thus, plays a crucial role. However, the main difference with halide systems is that significantly higher ionic dehydration penalty for Na⁺–DMPH association (by 21.24 kcal/mol) is almost *exactly* compensated by relative changes in the energy of ion–ion (–12.78 kcal/mol) and water–water (–7.72 kcal/mol) interactions (see Table 4). Similarly to halides, two latter types of interactions favor more the Na⁺–DMPH binding. We can

TABLE 5: Shares of the Ion–Ion ($\Delta\Delta E^{ii}$) and Water–Water ($\Delta\Delta E^{ss}$) Electrostatic Interactions, Favoring More Na⁺ Association with Cl[–] and DMPH Anion, Computed Relative to the Ion–Water ($\Delta\Delta E^{is}$) Electrostatic Interactions, Favoring More K⁺ Association with the above Anions^a

	$\Delta\Delta E^{ii}$	$\Delta\Delta E^{is}$	$\Delta\Delta E^{ss}$
NaCl – KCl	–50%	+100%	–31%
Na(DMPH) – K(DMPH)	–61%	+100%	–36%

^a Notations are the same as in Tables 3 and 4. Minus and plus signs at percentages mean favoring and disfavoring contributions, respectively, for Na⁺ association with Cl[–] and DMPH.

see from the Table 4 that overall difference between electrostatic (and van der Waals) energy changes for Na(DMPH) and K(DMPH) is nearly zero, suggesting that there is no energetic preference for the more effective K⁺ association with anion, caused by lower dehydration penalty, as in halides.

Another convenient way to present the main result of this section is to look at the shares of ion–ion and water–water electrostatic interactions, compensating the cation’s dehydration penalty in both types of systems, halide and DMPH solutions. These data are presented in the Table 5. The different extent of the counterbalancing the excess in sodium’s dehydration penalty ($\Delta\Delta E^{is}$) by the cation–anion ($\Delta\Delta E^{ii}$) and water–water ($\Delta\Delta E^{ss}$) interactions in halides and DMPH systems is clearly seen. In the latter systems, the Na–DMPH and the water–water interactions balance the unfavorable sodium’s dehydration by 11% and 5% more effectively, compared to halides. Larger difference between Na⁺ and K⁺ electrostatic interactions with Cl[–] and DMPH anion, respectively, can be rationalized by the smaller size of the oxygens in the DMPH’s phosphate group—the major binding sites of DMPH anion.

Next, we compare our findings—the picture of ionic behavior produced by the AMBER force-field, with the experimental data for ionic interactions in NaCl, KCl, NaH₂PO₄ and KH₂PO₄ electrolyte solutions. A finite concentration solution with significant ionic interactions may be compared with an ideal electrolyte solution at infinite dilution, where the latter is used to define the standard chemical potential.⁷¹ As the solution concentration is gradually increased, the average interionic distances decrease, where the resulting ion–ion interactions alter the solution free energy compared with the ideal solution. The corresponding change, the solution excess free energy, is characterized by the activity coefficient, γ . Next, we interpret the experimental activity coefficient curves for the NaCl, KCl, NaH₂PO₄ and KH₂PO₄ electrolyte solutions (see Figure 5) in the light of our energetic description of ionic association.

As expected from the Debye–Huckel theory, the activity coefficients of all electrolytes decrease initially as \sqrt{m} .⁷¹ The steeper initial decrease of the excess free energies for the potassium solutions, compared with the sodium solutions, may be rationalized by smaller hydration radius of K⁺.⁷¹ At some intermediate concentration, the activity coefficient curves go through a minimum, indicating an onset of unfavorable interactions (Figure 5). Interestingly, for NaCl this occurs at approximately 1 M, while for KCl the activity coefficient curve remains nearly flat above 2 M. Since at higher concentrations the ionic hydration shells start to overlap, the resulting dehydration penalty, which is larger for Na⁺ ions than for K⁺ ions, destabilizes more the NaCl solution. Our computer simulations, when using the AMBER force field, also indicated that K⁺ and Cl[–] association is more favorable, compared with Na⁺ and Cl[–] association. At the same time, it is important to note that the

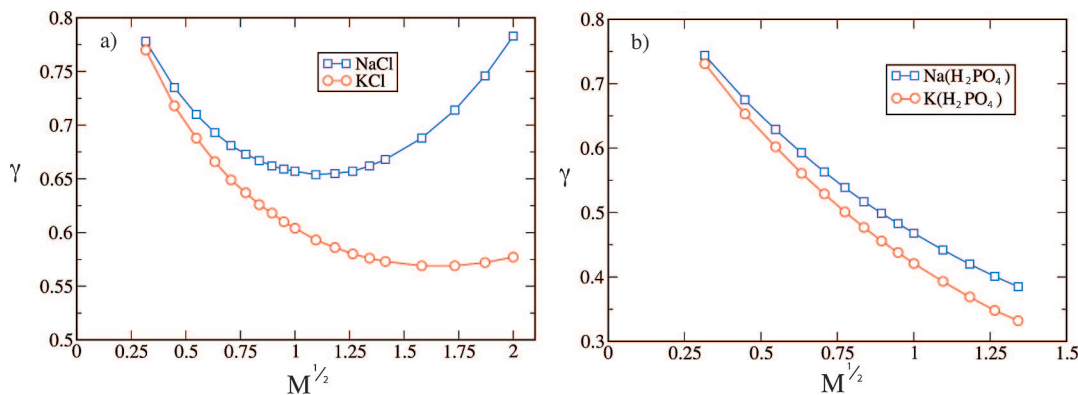


Figure 5. Experimentally measured activity coefficients γ , as a function of square root of molarity M , of electrolytes at 25 °C. Data for (a) NaCl, KCl and (b) NaH₂PO₄, KH₂PO₄ were drawn from tables in ref 71.

combined use of the Aquist's⁷² parameters for alkaline cations and Dang's⁷³ parameters for Cl⁻ was suggested to result in somewhat exaggerated KCl clustering in AMBER simulations.⁷⁴⁻⁷⁶ The way to reduce these inaccuracies of AMBER force-field was recently proposed.⁷⁶ Nevertheless, the obtained qualitative trends in the present study are consistent with the experiments on activity coefficient data (see Figure 5). In addition, noticeably stronger association of K⁺ and Cl⁻ compared with Na⁺ and Cl⁻, was shown from X-ray diffraction⁷⁷ and neutron diffraction experiments,⁷⁸ rationalizing lower solubility of KCl compared with NaCl.⁷⁷ This is in agreement with our computational findings. Similarly, our prediction of smaller difference between direct binding of Na⁺ and K⁺ to DMPH ion is also consistent with an experimentally observed smaller difference in activity coefficients for NaH₂PO₄ and KH₂PO₄ (Figure 5b). In summary, although it is clear that (perhaps modest) quantitative improvements to alkaline cations and chloride parameters are needed for the standard AMBER force field,^{74,76} and progress has been reported in this direction,⁷⁶ current parameters already allow to obtain trends that are in qualitative agreement with many experiments. This is further elaborated in the next section.

3.3. Survey of Relevant Experimental Results on the Ion–DNA Interactions. A set of experiments on compaction of long DNA chains, which is facilitated by monovalent counterions,⁴⁵⁻⁴⁷ may be interpreted to suggest greater Na⁺ association.⁴⁴ It was reported recently that DNA condensation, monitored by fluorescent microscopy, was mediated more significantly by Na⁺, than K⁺.⁴⁷ It should be noted, however, that the primary DNA compactor in the above experiment was the neutral poly ethylene glycol (PEG), used to mimic the crowded environment inside the living cell. Nevertheless, unequal concentrations of the added monovalent salts, NaCl or KCl, were then necessary to induce the DNA collapse. We speculate that stronger counterion association reduces electrostatic repulsion among DNA chains at close distances, thus, facilitating PEG-induced compaction. Since NaCl showed the higher activity than KCl, this argument suggests stronger Na⁺ association with DNA.

More recent experimental work reported by the same group has demonstrated that Na⁺ inhibits DNA compaction by spermidine (3+) significantly more strongly than K⁺.⁷⁹ In particular, half a amount of NaCl is needed, compared with KCl, to uncompact a DNA chain, which had previously been highly compacted by spermidine (3+). This uncompactation process may be naturally viewed as binding competition for DNA between the monovalent ions at very high abundance and spermidine (3+). Consequently, these results⁷⁹ suggest that the Na⁺ ions bind stronger to DNA compared with the K⁺ ions.

In an unrelated set of experiments, Parsegian group reported a direct measurement of forces between double-stranded DNA chains in ordered array solutions of different halides of monovalent cations.⁴⁸ These experiments revealed that the interchain forces, measured as a function of distance between DNA segments, increased by a factor of 2 as one passed from NaCl to KCl salt buffer. Thus, Na⁺ ions more effectively mitigate the electrostatic repulsion between DNA segments as they are brought in proximity, than K⁺. Furthermore, the authors analyzed their results in the context of Manning counterion condensation theory,²² finding that DNA charge neutralization by Na⁺ is ~20% larger than by K⁺.⁴⁸ This is in a good agreement with our results presented here (see Table 1). In addition, this experiment serves as a direct validation of our recently computed potentials of mean force (PMF) for bringing to proximity two DNA oligomers, in parallel orientation, in aqueous solution of NaCl and KCl salt buffers.⁷⁵ Our computed PMF in the NaCl buffer⁷⁵ turned out to be smaller than in the KCl buffer at all distances (0–20 Å) between DNA oligomers, consistent with the corresponding experimental findings.⁴⁸

The experimental trends described above are not completely consistent with the ones obtained from the NMR studies,¹⁶ where the K⁺ ions were found to have a slightly higher affinity toward binding to the DNA minor groove than the Na⁺ ions. In an earlier NMR studies on competitive binding of monovalent counterions to DNA, Record Jr. and co-workers found a slight preference of K⁺ binding over Na⁺.¹⁴ In yet another series of experimental publications on competition among mono-, di- and trivalent inorganic ions for association to oriented DNA fibers, lack of significant DNA selectivity was found toward the Na⁺ or K⁺ ions.^{19,20} In another recent experiment, the force was measured when electric field was applied to a DNA molecule placed in a nanopore.⁸⁰ Interestingly, the force was insensitive to changing the KCl buffer 50-fold, from 0.02 to 1 M KCl. In addition, the same force was measured in a 0.2 M NaCl buffer. Although a simple model suggested a 0.50 effective charge per DNA base pair in all these experiments, consistent with the Manning counterion condensation, we are not aware of a quantitative model explaining these experiments. Similar forces in NaCl and KCl buffers might indicate that K⁺ ions are trapped at a slightly larger distance beyond the third peak in the radial distribution function, compared with the Na⁺ ions. This, in turn, suggests that we should distinguish between counterion condensation, as in the Manning theory, from chemically specific association at close distances to DNA, which is the emphasis of our work.

Thus, on one hand, various experimental results on the relative extent of the Na⁺ and K⁺ association with DNA are not in

complete agreement with each other. On the other hand, it is likely that experiments on systems with finite DNA concentration^{48,79} probe different aspects of DNA electrostatics compared with experiments carried out in very dilute DNA solutions.⁸⁰ Further experimental investigations are needed to clarify these differences, and help to validate the accuracy of computational predictions.

4. Conclusions

In the present work, we explore the connection between the distinct behavior of various mobile ions in biological environments and the generic properties of electrolyte solutions. Specifically, we have studied the competitive Na⁺ vs K⁺ association with the 16-mer DNA oligomer solvated in explicit water by means of all-atom MD simulations. As opposed to the approaches used in our prior analysis of the same system,⁴⁴ here we probed the idea that the local interactions between mobile ions and the oppositely charged DNA phosphate groups primarily determine the higher association of Na⁺ counterions with the whole DNA chain. We addressed this question since a more general hypothesis, based on the empirical model of chaotropic vs kosmotropic ionic behavior in bioenvironments, states that ions in aqueous solutions are discriminated by the so-called Law of Matching Water Affinities.^{40–42} This means that oppositely charged ions or biomolecular ionic groups with matching values of hydration energies tend to associate. Particularly, this argument was used to rationalize the observed specificity of Na⁺ and K⁺ association with negatively charged biomolecular surfaces. For example, it was shown very recently that this hypothesis was well-suited for explaining the distinct Na⁺ and K⁺ interactions with some proteins, since the dominant role in noticeably higher Na⁺ association with these proteins was played by the effective local associations of sodium ions with the protein carboxylate groups.^{38,43}

One of the main conclusions of this work is that the above idea does not fully explain the observed higher affinity for Na⁺ toward DNA. This is because the dimethylphosphate (DMPH) anion, the dominant binding site for both Na⁺ and K⁺, exhibits negligible selectivity toward Na⁺ and K⁺. Our molecular dynamics simulations indicate that the *collective* effect of DNA charges drives both, the higher direct binding of Na⁺ to polyanion and also stronger condensation of Na⁺ within a region of ~9 Å from the DNA surface, coinciding with the Manning radius.²¹ Interestingly, in our recent detailed study of Na⁺ and K⁺ distributions around the same 16-base-pair DNA oligomer⁴⁴ we analyzed separately the halide-containing and halide-free DNA solutions. However, while in the former system the higher Na⁺ association was partially rationalized by the interplay between co-ion-counterion complexation and the DNA-counterion interactions,^{44,69} in a halide-free DNA solution the distinct sodium and potassium behavior was not completely understood. It follows from the present study that the enhanced anionic charge density, arising from the *polymeric* nature of DNA chain, is another mechanism that provides discrimination between Na⁺ and K⁺ in DNA solutions and is substantially responsible for higher Na⁺ absorption on DNA in the absence of extra halides.

Investigating the origin of dramatically different Na⁺ and K⁺ association with DMPH and Cl⁻ anions demonstrated how ion-DNA interactions in salt aqueous medium can be understood from studying simple ionic pairing, i.e., from properties of electrolyte solutions. In particular, we analyzed the free energy changes upon Na⁺ and K⁺ binding to chloride and DMPH anions. It was shown that different dehydration penalties of Na⁺ and K⁺ ions play a primary role in determining the noticeable

difference between K⁺-Cl⁻ and Na⁺-Cl⁻ pairings. On the other hand, this difference is counterbalanced by different types of microscopic interactions upon association of Na⁺ and K⁺ with DMPH anion. As mentioned above, the latter results in the unnoticeable selectivity for DNA building block, the DMPH anion, toward Na⁺ and K⁺ ions. Thus, in the halide-containing DNA solutions both, the different dehydration penalty of monovalent counterions and the DNA polyionic nature, produce noticeably higher Na⁺ association with DNA.

In summary, our AMBER simulations indicate stronger association of Na⁺ with DNA, compared to K⁺. We have found that this effect is significantly driven by the polyionic nature of DNA, a collective effect, which is the main result of this work. Our CHARMM simulations also point to this polyionic effect, however, the difference between Na⁺ and K⁺ association is markedly reduced compared with the AMBER results. A different sodium and potassium dehydration penalty appeared to be one of the main microscopic mechanisms explaining stronger Na⁺ condensation on DNA in the halide-containing DNA solutions in AMBER simulations. Our computational predictions are consistent with several DNA experiments in NaCl and KCl buffers, including experiments by Yoshikawa^{45–47,79} and Parsegian⁴⁸ groups, as well as with an experimentally measured activity coefficients for NaCl, KCl, NaH₂PO₄ and KH₂PO₄ electrolyte solutions.⁷¹ On the other hand, some other experiments, including NMR spectroscopy and force measurements,^{16,14} do not find a substantial difference between the Na⁺ and K⁺ binding to DNA. Thus, further experimental and computational works are needed to clarify the reasons for the disagreements between various experiments. In particular, it is desirable to explore whether different experiments probe different aspects of mobile counterion condensation in DNA solutions that are either very dilute or at a finite DNA concentration. Finally, these experiments and our current analysis may indicate that different counterions might have somewhat different associated Manning radii—a computational strategy to identify these radii from atomistic simulations will be helpful.

Acknowledgment. We are grateful to Dr. Gerald Manning for bringing to our attention ref 80 and providing an interpretation of these finding in the context of our results. We thank Dr. Alexander Grosberg, Dr. Gilbert Nathanson, Dr. Michael Rubinstein, Dr. Johan Ulander, Dr. Kenichi Yoshikawa, Dr. Anatoly Zinchenko, and Pavel Zhuravlev for helpful discussions. We gratefully acknowledge support from the North Carolina Biotechnology Center (NCBC) Grant No. 2006-MRG-1107 and the Arnold and Mabel Beckman Foundation Beckman Young Investigator Award.

References and Notes

- (1) Saenger, W. *Principles of nucleic acid structure*; Springer: New York, 1984.
- (2) van Holde, K. E. *Chromatin*; Springer: New York, 1989.
- (3) Alberts, B.; Johnson, A.; Lewis, J.; Raff, M.; Roberts, K.; Walter, P. *Molecular biology of the cell*; Garland Science: London, 2002.
- (4) Koculi, E.; Thirumalai, D.; Woodson, S. A. *J. Mol. Biol.* **2006**, *359*, 446–454.
- (5) Koculi, E.; Hyeon, C.; Thirumalai, D.; Woodson, S. A. *J. Am. Chem. Soc.* **2007**, *129*, 2676–2682.
- (6) Lund, M.; Jonsson, B. *Biophys. J.* **2003**, *85*, 2940–2947.
- (7) Chodankar, S.; Aswal, V. K. *Phys. Rev. E* **2005**, *72*, 041931.
- (8) Tavares, F. W.; Bratko, D.; Blanch, H. W.; Prausnitz, J. M. *J. Phys. Chem. B* **2004**, *108*, 9228–9235.
- (9) Shui, X.; Sines, C. C.; McFail-Isom, L.; VanDerveer, D.; Williams, L. D. *Biochemistry* **1998**, *37*, 16877–16887.
- (10) Shui, X.; McFail-Isom, L.; Hu, G. G.; Williams, L. D. *Biochemistry* **1998**, *37*, 8341–8355.

- (11) Chiu, T. K.; Kaczor-Grzeskowiak, M.; Dickerson, R. E. *J. Mol. Biol.* **1999**, *292*, 589–608.
- (12) Tereshko, V.; Minasov, G.; Egli, M. *Nucleic Acids Res.* **1999**, *121*, 3590–3595.
- (13) Tereshko, V.; Wilds, C. J.; Minasov, G.; Prakash, T. P.; Maier, M. A.; Howard, A.; Wawrzak, Z.; Manoharan, M.; Egli, M. *Nucleic Acids Res.* **2001**, *29*, 1208–1215.
- (14) Bleam, M. L.; Anderson, C. F.; Record, M. T. *Proc. Natl. Acad. Sci. U.S.A.* **1980**, *77*, 3085–3089.
- (15) Halle, B.; Denisov, V. P. *Biopolymers* **1998**, *48*, 210–233.
- (16) Denisov, V. P.; Halle, B. *Proc. Natl. Acad. Sci. U.S.A.* **2000**, *97*, 629–633.
- (17) Hud, N. V.; Feigon, J. *Biochemistry* **2002**, *41*, 9900–9910.
- (18) Marincola, F. C.; Denisov, V. P.; Halle, B. *J. Am. Chem. Soc.* **2004**, *126*, 6739–6750.
- (19) Korolev, N.; Lyubartsev, A. P.; Rupprecht, A.; Nordenskiöld, L. *Biophys. J.* **1999**, *77*, 2736–2749.
- (20) Korolev, N.; Lyubartsev, A. P.; Rupprecht, A.; Nordenskiöld, L. *Biopolymers* **2001**, *58*, 268–278.
- (21) Manning, G. S. *J. Chem. Phys.* **1969**, *51*, 924–933.
- (22) Manning, G. S. *Q. Rev. Biophys.* **1978**, *11*, 179–246.
- (23) Shklovskii, B. I. *Phys. Rev. Lett.* **1999**, *82*, 3268–3271.
- (24) Naji, A.; Netz, R. R. *Eur. Phys. J. E: Soft Matter* **2004**, *13*, 43–59.
- (25) Lee, K.-C.; Borukhov, I.; Gelbart, W. M.; Liu, A. J.; Stevens, M. J. *Phys. Rev. Lett.* **2004**, *93*, 128101.
- (26) Angelini, T. E.; Liang, H.; Wriggers, W.; Wong, G. C. L. *Proc. Natl. Acad. Sci. U.S.A.* **2003**, *100*, 8634–8637.
- (27) Fuoss, R. M.; Katchalsky, A.; Lifson, S. *Proc. Natl. Acad. Sci. U.S.A.* **1951**, *37*, 579–589.
- (28) Shkel, I. A.; Tsodikov, O. V.; Record, M. T. *Proc. Natl. Acad. Sci. U.S.A.* **2002**, *99*, 2597–2602.
- (29) Deshkovski, A.; Obukhov, S.; Rubinstein, M. *Phys. Rev. Lett.* **2001**, *86*, 2341–2344.
- (30) Cheatham, T. E.; Young, M. A. *Biopolymers* **2000**, *56*, 232–256.
- (31) Cheatham, T. E.; Kollman, P. A. *Annu. Rev. Phys. Chem.* **2000**, *51*, 435–471.
- (32) Egli, M. *Chem. Biol.* **2002**, *9*, 277–286.
- (33) Laughton, C.; Luque, F.; Orozco, M. *J. Phys. Chem.* **1995**, *99*, 11591–11599.
- (34) Rueda, M.; Cubero, E.; Laughton, C. A.; Orozco, M. *Biophys. J.* **2004**, *87*, 800–811.
- (35) Ponomarev, S. Y.; Thayer, K. M.; Beveridge, D. L. *Proc. Natl. Acad. Sci. U.S.A.* **2004**, *101*, 14771–14775.
- (36) Varnai, P.; Zakrzewska, K. *Nucleic Acids Res.* **2004**, *32*, 4269–4280.
- (37) Randall, G. L.; Pettitt, B. M.; Buck, G. R.; Zechiedrich, E. L. *J. Phys.: Condens. Matter* **2006**, *18*, S173–S185.
- (38) Vrbka, L.; Vondrasek, J.; Jagoda-Cwiklik, B.; Vacha, R.; Jungwirth, P. *Proc. Natl. Acad. Sci. U.S.A.* **2006**, *103*, 15440–15444.
- (39) Darnel, J.; Lodish, H.; Baltimore, D. *Molecular Cell Biology*; Scientific American Books: New York, 1990.
- (40) Collins, K. D. *Biophys. J.* **1997**, *72*, 65–76.
- (41) Collins, K. D. *Methods* **2004**, *34*, 300–311.
- (42) Collins, K. D. *Biophys. Chem.* **2006**, *119*, 271–281.
- (43) Jagoda-Cwiklik, B.; Vacha, R.; Lund, M.; Srebro, M.; Jungwirth, P. *J. Phys. Chem. B* **2007**, *111*, 14077–14079.
- (44) Savelyev, A.; Papoian, G. A. *J. Am. Chem. Soc.* **2006**, *128*, 14506–14518.
- (45) Mayama, H.; Iwataki, T.; Yoshikawa, K. *Chem. Phys. Lett.* **2000**, *318*, 113–117.
- (46) Mayama, H.; Yoshikawa, K. *Macromol. Symp.* **2000**, *160*, 55–60.
- (47) Zinchenko, A. A.; Yoshikawa, K. *Biophys. J.* **2005**, *88*, 4118–4123.
- (48) Podgornik, R.; Rau, D. C.; Parsegian, V. A. *Biophys. J.* **1994**, *66*, 962–971.
- (49) Feig, M.; Pettitt, B. M. *Biophys. J.* **1999**, *77*, 1769–1781.
- (50) McConnell, K. J.; Beveridge, D. L. *J. Mol. Biol.* **2000**, *304*, 803–820.
- (51) Hamelberg, D.; McFail-Isom, L.; Williams, L. D.; Wilson, W. D. *J. Am. Chem. Soc.* **2000**, *122*, 10513–10520.
- (52) Lyubartsev, A. P.; Laaksonen, A. *J. Biomol. Struct. Dyn.* **1998**, *16*, 579–592.
- (53) Cheng, Y.; Korolev, N.; Nordenskiöld, L. *Nucleic Acids Res.* **2006**, *34*, 686–696.
- (54) Vaitheeswaran, S.; Thirumalai, D. *J. Am. Chem. Soc.* **2006**, *128*, 13490–13496.
- (55) Miyamoto, S.; Kollman, P. A. *J. Comput. Chem.* **1992**, *13*, 952–962.
- (56) Case, D.; Cheatham, T.; Darden, T.; Gohlke, H.; Luo, R.; Merz, K.; Onufriev, A.; Simmerling, C.; Wang, B.; Woods, R. J. *Comput. Chem.* **2005**, *26*, 1668–1688.
- (57) Wang, J.; Cieplak, P.; Kollman, P. J. *Comput. Chem.* **2000**, *21*, 1049–1074.
- (58) Shields, G. C.; Laughton, C. A.; Orozco, M. *J. Am. Chem. Soc.* **1998**, *120*, 5895–5904.
- (59) Berendsen, H. J.; Postma, J. P.; van Gunsteren, W. F.; DiNola, A.; Haak, J. R. *J. Chem. Phys.* **1984**, *81*, 3684–3690.
- (60) Ryckaert, J.-P.; Ciccotti, G.; Berendsen, H. J. *J. Comput. Phys.* **1977**, *23*, 327–341.
- (61) Darden, T.; York, D.; Pedersen, L. *J. Chem. Phys.* **1993**, *98*, 10089–10092.
- (62) Barrat, J.-L.; Hansen, J.-P. *Basic concepts for simple and complex liquids*; Cambridge University Press: Cambridge, 2003.
- (63) Kohlbacher, O.; Lenhof, H. P. *Bioinformatics* **2000**, *16*, 815–824.
- (64) Liu, W.; Wood, R. H.; Doren, D. J. *J. Chem. Phys.* **2003**, *118*, 2837.
- (65) Chen, A. A.; Pappu, R. V. *J. Phys. Chem. B* **2007**, *111*, 6469–6478.
- (66) Patra, M.; Karttunen, M. *J. Comput. Chem.* **2004**, *25*, 678–689.
- (67) MacKerell, A. D.; B. N.; N. F., Jr. *Biopolymers* **2001**, *56*, 257–265.
- (68) Brooks, B. R.; Brucoleri, R. E.; Olafson, B. D.; States, D. J.; Swaminathan, S.; Karplus, M. *J. Comput. Chem.* **1983**, *4*, 187–217.
- (69) Savelyev, A.; Papoian, G. A. *Mendeleev Commun.* **2007**, *17*, 97–99.
- (70) Finkelstein, A. V.; Ptitsyn, O. B. *Protein physics*; Academic Press: New York, 2002.
- (71) Robinson, R. A.; Stokes, R. H. *Electrolyte solutions*; Dover Publications, Inc.: Mineola, NY, 2002.
- (72) Aquist, J. *J. Phys. Chem.* **1990**, *94*, 8021–8024.
- (73) Smith, D. E.; Dang, L. X. *J. Chem. Phys.* **1993**, *100*, 3757–3766.
- (74) Auffinger, P. C. T. E. C. V. A. *J. Chem. Theory Comput.* **2007**, *3*, 1851–1859.
- (75) Savelyev, A.; Papoian, G. A. *J. Am. Chem. Soc.* **2007**, *129*, 6060–6061.
- (76) Chen, A. A.; Pappu, R. V. *J. Phys. Chem. B* **2007**, *111*, 11884–11887.
- (77) Ohtaki, H.; Fukushima, N. *J. Solution Chem.* **1992**, *21*, 23–38.
- (78) Mancinelli, R.; Botti, A.; Bruni, F.; Ricci, M. A.; Soper, A. K. *J. Phys. Chem. B* **2007**, *111*, 13570–13577.
- (79) Hibino, K.; Yoshikawa, Y.; Murata, S.; Saito, T.; Zinchenko, A. A.; Yoshikawa, K. *Chem. Phys. Lett.* **2006**, *426*, 405–409.
- (80) Keyser, U. F.; Koeleman, B. N.; Dorp, S. V.; Krapf, D.; Smeets, R. M. M.; Lemay, S. G.; Dekker, N. H.; Dekker, C. *Nat. Phys.* **2006**, *2*, 473–477.